Vibrational spectra of lead tetraborate: experimental and theoretical analysis

2007 J. Phys.: Condens. Matter 19 436207

(http://iopscience.iop.org/0953-8984/19/43/436207)

IOP PUBLISHING JOURNAL OF PHYSICS: CONDENSED MATTER

J. Phys.: Condens. Matter **19** (2007) 436207 (11pp) doi:10.1088/0953-8984/19/43/436207

Vibrational spectra of lead tetraborate: experimental and theoretical analysis

Yufang Wang[1,4], Min Feng[1], Hui Wang[1], Peizhen Fu[2], Junxin Wang[3], Xuewei Cao[1] and Guoxiang Lan[1]

[1] Department of Physics, Nankai University, Tianjin 300071, People's Republic of China
[2] Beijing Center for Crystal Research and Development, Technical Institute of Physics and Chemistry, Chinese Academy of Sciences, Beijing 100080, People's Republic of China
[3] School of Earth and Space Sciences, University of Science and Technology of China, Hefei, Anhui 230026, People's Republic of China

E-mail: yfwang@nankai.edu.cn

Received 3 June 2007, in final form 4 September 2007
Published 26 September 2007
Online at stacks.iop.org/JPhysCM/19/436207

Abstract

Raman and infrared reflectance spectra of single-crystal lead tetraborate (PbB_4O_7:PTB) have been recorded. Using a first-principles calculation, the phonon dispersion relation of PTB has been derived within the local density approximation. A symmetry analysis of the phonon modes at the centre of Brillouin zone was performed, and calculated frequencies are compared to experimental spectra. A good agreement between calculated and measured frequencies was obtained.

(Some figures in this article are in colour only in the electronic version)

1. Introduction

Over the past few decades, a detailed knowledge of the vibrational spectra of important nonlinear optical borate crystals β-BaB_2O_4 (BBO), LiB_3O_5 (LBO), $CsLiB_6O_{10}$ (CLBO) and CsB_3O_5 (CBO) has been obtained [1–5]. The special performances of these new borate-based nonlinear optical crystals are their superior transparency at wavelengths below 200 nm and excellent resistance to optical damage. BBO and LBO are now widely applied in second-harmonic generation and optical parametric oscillation. Lead tetraborate (PbB_4O_7:PTB) is a new nonlinear optical crystal. PTB has advantages over existing nonlinear optical crystals such as relatively straightforward growth, transparency at wavelengths above 300 nm, higher optical nonlinearity, and higher refractive index relative to other borates [6]. These properties are related to the unique tetrahedral boron–oxygen coordination in PTB. It is important to study the influence of different borate groups on the properties of the corresponding crystals.

[4] Author to whom any correspondence should be addressed.

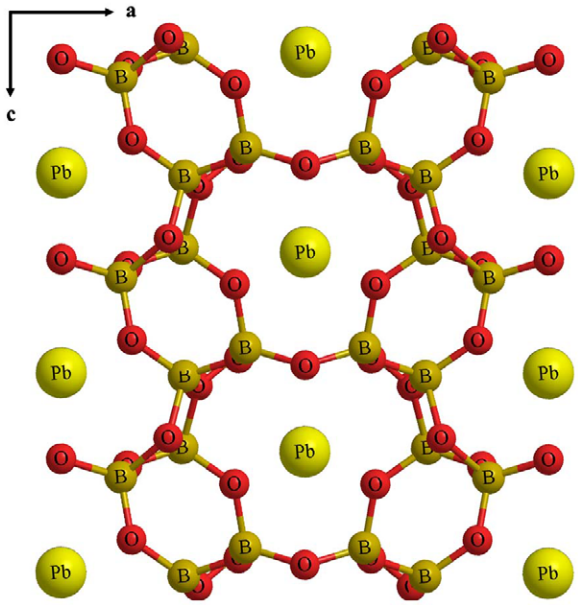

Figure 1. A projection on (010) showing the channels in the structure by the network of corner-sharing BO_4-tetrahedra. The lead atoms lie in the channels.

Vibrational spectroscopy can be an important tool in understanding the chemical bonding, and it may provide insights that can be used in an empirical way in the evaluation of the nonlinear optical properties. In the present work, we present our theoretical results of the phonon dispersion of PTB using density-functional theory (DFT). The observed polarized Raman and infrared frequencies of PTB are analysed and assigned by comparison to the computed values. The experimental and calculated results are in good agreement.

2. Crystal structure and theoretical analysis

Lead tetraborate is isostructural with strontium tetraborate (SrB_4O_7). The crystal structures of those compounds have been analysed by Perloff *et al* [7]. More accurate bond lengths and angles of PTB have been determined and refined by Corker *et al* [8] using single-crystal x-ray diffraction data. PTB crystallizes in a complex orthorhombic cell with two formula units per cell. The space group is $Pmn2_1$, with unit cell dimensions $a = 1.0860$ nm, $b = 0.4463$ nm and $c = 0.4251$ nm [8]. There are four inequivalent O sites, one of which, O(1), together with the Pb atom, is situated on a mirror plane at $x = 0$. The remaining atoms are all on general positions. The nearest-neighbour distances vary from 0.144 to 0.156 nm for the B–O bond, and from 0.248 to 0.289 nm for the Pb–O bond. The crystal structure of PTB consists of a three-dimensional borate network, which contains channels along the [010] direction (figure 1). The Pb atoms fit into these channels. All boron atoms are tetrahedrally coordinated and all tetrahedra are corner sharing.

We use the factor group analysis method to classify the vibrational modes of PTB. The factor group of the Γ point in the Brillouin zone of PTB crystal is isomorphic with point group C_{2v}. The characters $\chi_q^{(i)}(R)$ of the irreducible representation of the C_{2v} point group,

Table 1. Characteristics of the reducible and irreducible representations of the C_{2v} point group.

C_{2v}	E	C_2	σ_y	σ_x	
$\{R\|\tau_R\}$	$\{E\|0\}$	$\{C_2\|0\frac{1}{2}\frac{1}{2}\}$	$\{\sigma_y\|0\frac{1}{2}\frac{1}{2}\}$	$\{\sigma_x\|000\}$	
A_1	1	1	1	1	$T_z x^2 y^2 z^2$
A_2	1	1	−1	−1	xy
B_1	1	−1	1	−1	$T_x xz$
B_2	1	−1	−1	1	$T_y yz$
$U_{(R,\tau_R)}$	24	0	0	4	
$\pm 1 + 2\cos\theta_R$	3	−1	1	1	
$\chi(R)$	72	0	0	4	

the representation operations (R, τ_R), and the number of atoms $U_{(R,\tau_R)}$ in the primitive cell which remain invariant under the operation (R, τ_R) are listed in table 1.

The calculated results indicate that there are $19A_1 + 17A_2 + 17B_1 + 19B_2$ vibrational modes, including three acoustic modes, $A_1 + B_1 + B_2$. Among the optical modes $18A_1 + 17A_2 + 16B_1 + 18B_2$, the A_1, B_1 and B_2 modes are polar phonons, and are both infrared and Raman active. The A_2 modes are nonpolar phonons and are only Raman active.

3. Experimental and calculated method

The PTB crystal was grown by the Kyropoulos method at the University of Science and Technology of China. The structure of the PTB crystal was analysed by x-ray diffraction, and no trace of water was found. The results are in agreement with those of [7]. A PTB single crystal measuring 11 mm × 8.5 mm × 4.7 mm along the a, b and c axes was cut perpendicular to these axes. We define the x, y and z axes to be collinear with the crystal a, b and c axes. The crystal surfaces were polished to optical quality for infrared (IR) reflectance and Raman scattering experiments.

Ar^+-ion laser radiation (514.5 nm, 0.1 W) was used to excite Raman spectra, and the scattered light was analysed with a Spex-1403 double monochromator. The slit widths of the entrance and exit were 200 μm, which resulted in a resolution of $\leqslant 2$ cm^{-1}. The Raman spectra were recorded from 10–1200 cm^{-1} with a scanning step of 1 cm^{-1} in the scattering configurations $x(zz)y$, $x(yx)y$, $y(zx)z$, $x(zy)z$ and $z(xx)\bar{z}$, corresponding to A_1(TO), A_2, B_1(TO), B_2(TO) and A_1(LO) vibrational modes, respectively. There we use the usual Porto notation $a(cd)b$, where a and b are the direction of the incident and scattered radiation, respectively, and c and d are the polarized directions of the incident and scattered light, respectively.

The infrared reflectance spectra were recorded on a Nicolet 560 E.S.P. Fourier transform infrared spectrometer with resolution 4 cm^{-1}, covering the range 470–4000 cm^{-1}. The infrared reflectance spectra of the A_1, B_1 and B_2 vibrational modes were obtained with the polarization of incident light parallel to the z-axis, x-axis and y-axis, respectively.

A first-principles method based on density-functional theory (DFT) [9] and the local density approximation (LDA) [10] were used in our study to calculate the phonon dispersion curves of PTB crystal. In our total-energy calculations and corresponding structure optimizations, we used the plane-wave basis DFT pseudopotential method [11]. The ion potentials were described by the norm-conserving pseudopotentials proposed by Hamann [12, 13]. The Monkhorst and Pack scheme of k-point sampling was used for integration over the first Brillouin zone [14].

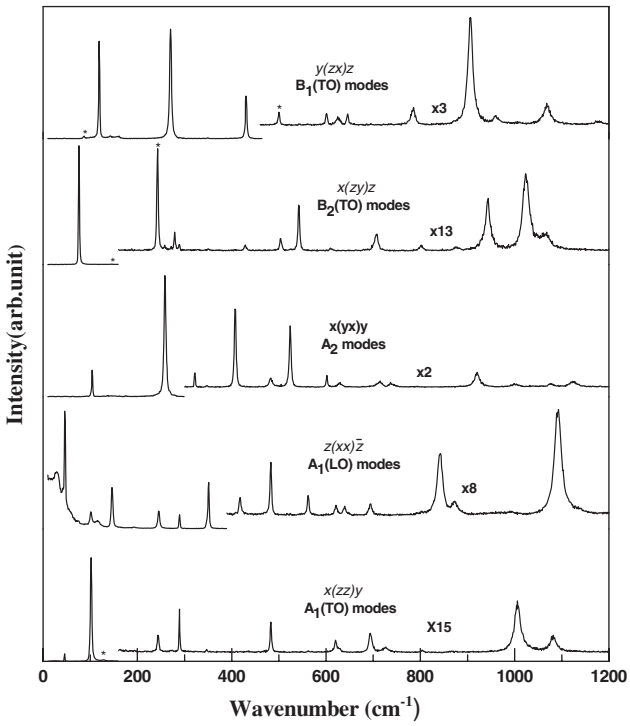

Figure 2. Raman spectra of PTB crystal in various configurations at room temperature, corresponding to $A_1(TO)[x(zz)y]$, $A_1(LO)[z(xx)(-z)]$, $A_2[x(yx)y]$, $B_1(TO)[y(zx)z]$, and $B_2(TO)[x(zy)z]$. The peak positions (full-widths at half-maximum: FWHMs) of the strongly excited modes are observed at 46(3), 76(3), 102(3), 119(3), 258(4), and 270(4) cm^{-1}, respectively. The leakage modes are indicated by an asterisk.

4. Results and discussion

4.1. Raman spectra

The Raman spectra of PbB_4O_7 crystal are shown in figure 2. There is a well-defined gap between the lower-wavenumber group of lines and higher-wavenumber groups, although the excitation spectrum of PTB is more complex (for detailed discussions see later). A few bands are attributed to leakages of some vibrational modes, which are mainly connected with the wide divergence angles of the incident light and collecting angles of the scattered light. The frequencies of the observed Raman bands are listed in tables 2 and 3, together with the theoretical results. It can be seen that the number of observed Raman bands roughly agrees with group theoretical predictions.

4.2. Infrared spectra

The polarized infrared reflectance spectra of the $A_1(z)$, $B_1(x)$ and $B_2(y)$ modes of PTB crystal are shown in figure 3. By using the Kramers–Kronig technique, we obtained the dispersions curves of the refractive index, $n(\omega)$, extinction coefficient, $k(\omega)$, and the real and imaginary parts of the reciprocal of the dielectric coefficient, $(1/\varepsilon)_i$. From the dispersion curves of $\varepsilon_i(\omega)$ and $(1/\varepsilon)_i$ the transverse and longitudinal frequencies of the polar modes, ω_{TO} and ω_{LO}, were

Table 2. Experimental and calculated frequencies (cm^{-1}) of the A_1 and A_2 vibrational modes (Note: Relative intensity: vs = very strong, s = strong, m = medium, w = weak, vw = very weak.)

A_1 modes					A_2 modes	
Raman		IR				
TO	LO	TO	LO	Cal.	Raman	Cal.
		1142s	1238	1157	1126vw	1145
1082w	1092w	1082w	1093	1081	1077vw	1080
				1026		1039
1006w	1067vw	1004s	1068	998	999vw	1023
868vw	873vw	868w	872	878	921vw	920
804vw	842w	806s	847	791		784
727vw		725s	794	749	737vw	754
694vw	695vw			689	717vw	714
628vw	640vw	623m	640	636	629vw	639
620vw	621vw			602	602vw	582
562vw	562vw			554	524w	517
483w	483w			475	483vw	483
418vw	418vw			408	407w	408
347vw	351m			337	322vw	316
289w	289w			291	258s	262
244vw	245w			252		178
102s	146s			113	104w	101
46m	46s			49		

Table 3. Experimental and calculated frequencies (cm^{-1}) of the B_1 and B_2 vibrational modes. (Note: Relative intensity: vs = very strong, s = strong, m = medium, w = weak, vw = very weak.)

B_1 modes				B_2 modes			
Raman	IR			Raman	IR		
TO	TO	LO	Cal.	TO	TO	LO	Cal.
1178vw	1217s	1338	1192				1336
1068vw	1072w	1082	1082	1064vw	1074	1205	1081
1006vw	1003s	1059	1002	1023vw	1028	1049	1026
960vw	966vw	968	956	944vw	935	977	944
907m			909				936
881vw	879m	893	865	876vw	879	901	885
786vw	787m	793	796	802vw			808
			783		784	839	786
646vw	650s	660	640	708vw	705	721	702
625vw	629w	632	632	609vw	609	617	598
602vw	602w	604	592	542vw	541	548	533
430m			423	504vw	505	505	494
270s			277				494
			248	429vw			421
143vw			166	289vw			289
119s			101	279vw			279
				76s			78
				63vw			71

determined respectively. The results are also listed in tables 2 and 3. The three principal refractive indices of PTB at 2500 cm^{-1} were determined from the $n(\omega)$ dispersion curves, and

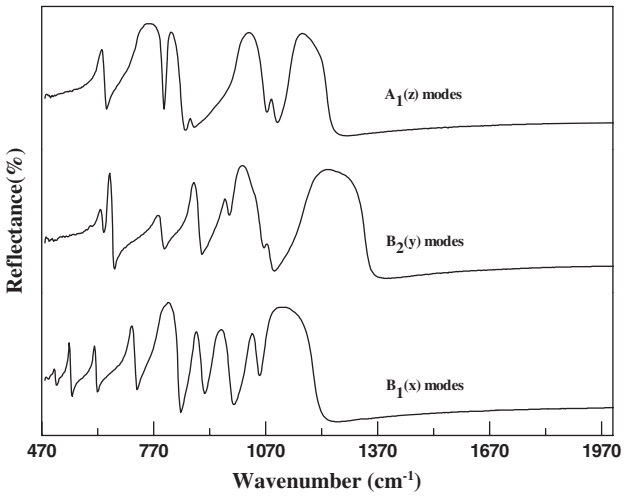

Figure 3. Infrared reflectance spectra of $A_1(z)$, $B_2(y)$ and $B_1(x)$ modes of PTB crystal at room temperature, obtained with the polarization of incident light parallel to the z-axis, y-axis and x-axis, respectively.

the results are $n_x = 1.9937, n_y = 1.9275$ and $n_z = 1.9481$, which are consistent with the result in [6].

It must be noticed that this method requires the knowledge of the reflectivity as a function of frequency from zero to infinity. Usually one can obtain the low-frequency and high-frequency reflectance spectra by extrapolations. However, we simply obtained the reflectance spectra from 400–4000 cm^{-1}; this deficiency will give rise to some errors. But the transverse and longitudinal frequencies of the A_1 modes, determined from experimental Raman spectra and Kramer–Kronig relations respectively, are in reasonable agreement.

4.3. Phonon dispersion

Figure 4 shows the Brillouin zone (BZ) and phonon dispersion curves of PTB crystal along the most important axes within and on the surface of the BZ. It can be seen that there exists a band gap which separates the high-energy bands from inner rigid vibrations of basic groups of PTB. From the calculated results we can perform a symmetry analysis by comparing the basis functions of the irreducible representations with the eigenvectors resulting from the dynamical matrix. Both the calculated frequencies and species of each vibrational mode at the Γ point are listed in tables 2 and 3.

A few frequencies predicted from the calculation are absent in the experimental spectra, probably because of their small intensities. As can be seen from tables 2 and 3, a good agreement between most theoretical and experimental vibrational modes is obtained. In general the deviation from experimental results is 2–24 cm^{-1}. The maximal difference between the experimental and measured frequencies is 24 cm^{-1} for the scattering band of the A_2 mode at 999 cm^{-1}.

4.4. Mode assignments

For many crystals, the types of vibrational mode can be divided into two parts: external and internal modes. The external modes are composed of both translational and librational modes. Internal modes are vibrations which can be associated with those of a molecular unit, shifted

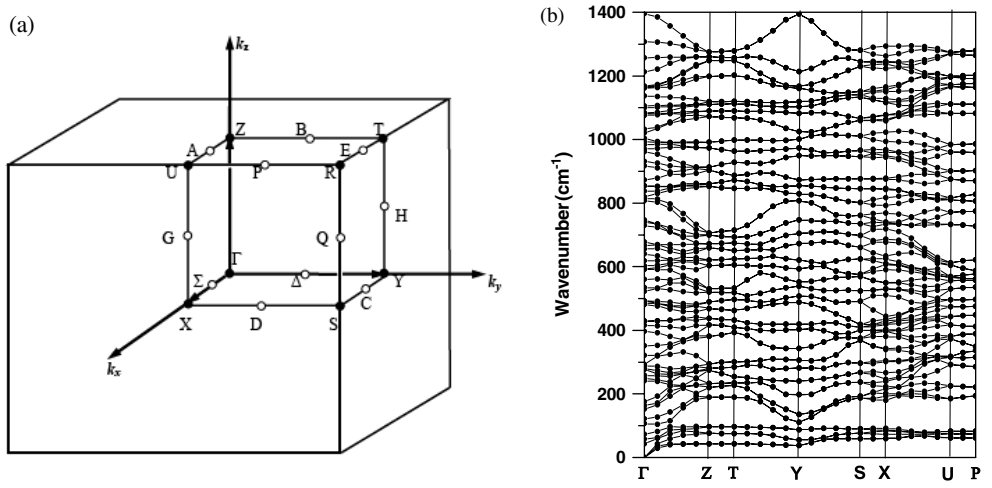

Figure 4. (a) Brillouin zone and (b) calculated phonon dispersion of PTB crystal.

by its interaction within the structure. This is valid in the case where the internal and external vibration frequencies differ considerably. As previously mentioned, the structure of PTB crystal is a three-dimensional network; its basic structural units are not isolated.

Similarly to the partial phonon density of states, we determined the contribution from the given atom to each vibration at the Γ point: $N_j(\omega) = \sum_i |e_j(i)|^2 \delta(\omega - \omega_j(\Gamma))$. This concept can be used to analyse the vibrational modes. Figure 5 shows the contribution from atoms in the unit cell to vibrational modes at the Γ point.

The external modes comprise both translational and librational modes. For the PbB_4O_7 crystal, in the low-frequency region (about 0–200 cm^{-1}) the Raman bands are attributed to the translational motion of the mass centre of BO_4 and Pb ions and the hindered rotations (librations) of the BO_4 (or B_3O_9 six-membered ring). From figure 5 it can be seen that the Pb atoms mainly contribute to the vibrations with frequencies below 166 cm^{-1}.

The vibrational modes with calculated frequencies 49 cm^{-1} (A_1), 71 cm^{-1} (B_2) and 101 cm^{-1} (A_2) originate from the Pb atoms, where two Pb atoms in the unit cell vibrate out of phase along the y-axis, z-axis and x-axis, respectively. The corresponding Cartesian displacements of atoms are given in figures 6(a)–(c). The Raman scattering bands at 76 cm^{-1} (B_2), 119 cm^{-1} (B_1) and 102 cm^{-1} (A_1) originate from the Pb atoms and six-membered rings being out of phase, along the y-axis, x-axis and z-axis, respectively (see figures 6(d)–(f)). The corresponding calculated frequencies are 78, 101 and 113 cm^{-1}, respectively. Vibrational modes with calculated frequencies 166 and 178 cm^{-1} come from the libration vibrations of six-membered rings (see figures 7(a), (b)).

Zhigadlo *et al* [15] reported the infrared spectra of $Li_2B_4O_7$, in which the B and O atoms form a network of B_4O_7 groups and the Li atoms lie in a channel of very distorted tetrahedra. The characteristic vibrational peaks of Li coordinated by four O nearest neighbours occurred at 355 and 424 cm^{-1}, which are much higher than the characteristic vibrations of Pb atoms in the PTB crystal.

Figure 8 show the Cartesian displacements of atoms in some normal modes. It can be seen that the vibrational character of PTB crystal is very complexity. The vibrational bands with frequencies above 1100 cm^{-1} are mainly due to the B–O stretching vibration. Because of the complex character of vibrational modes we simply give the Cartesian displacements of atoms

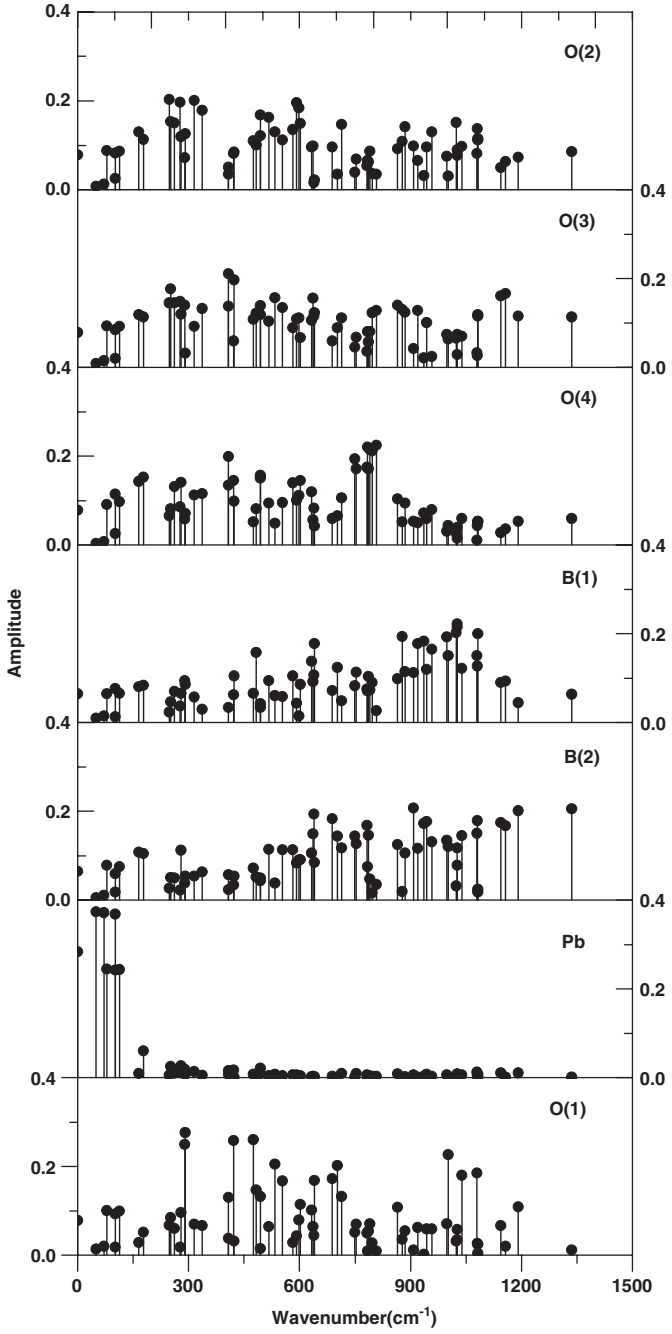

Figure 5. The contribution from atoms in the unit cell to vibrational modes at the Γ point.

in some normal modes of PTB (see figure 8). The reflectance band at about 1142 cm^{-1} is very strong (see figure 3, A_1 mode); the corresponding calculated frequency is 1157 cm^{-1}. From figure 8(d) we can see that it is associated with the B–O stretching vibration.

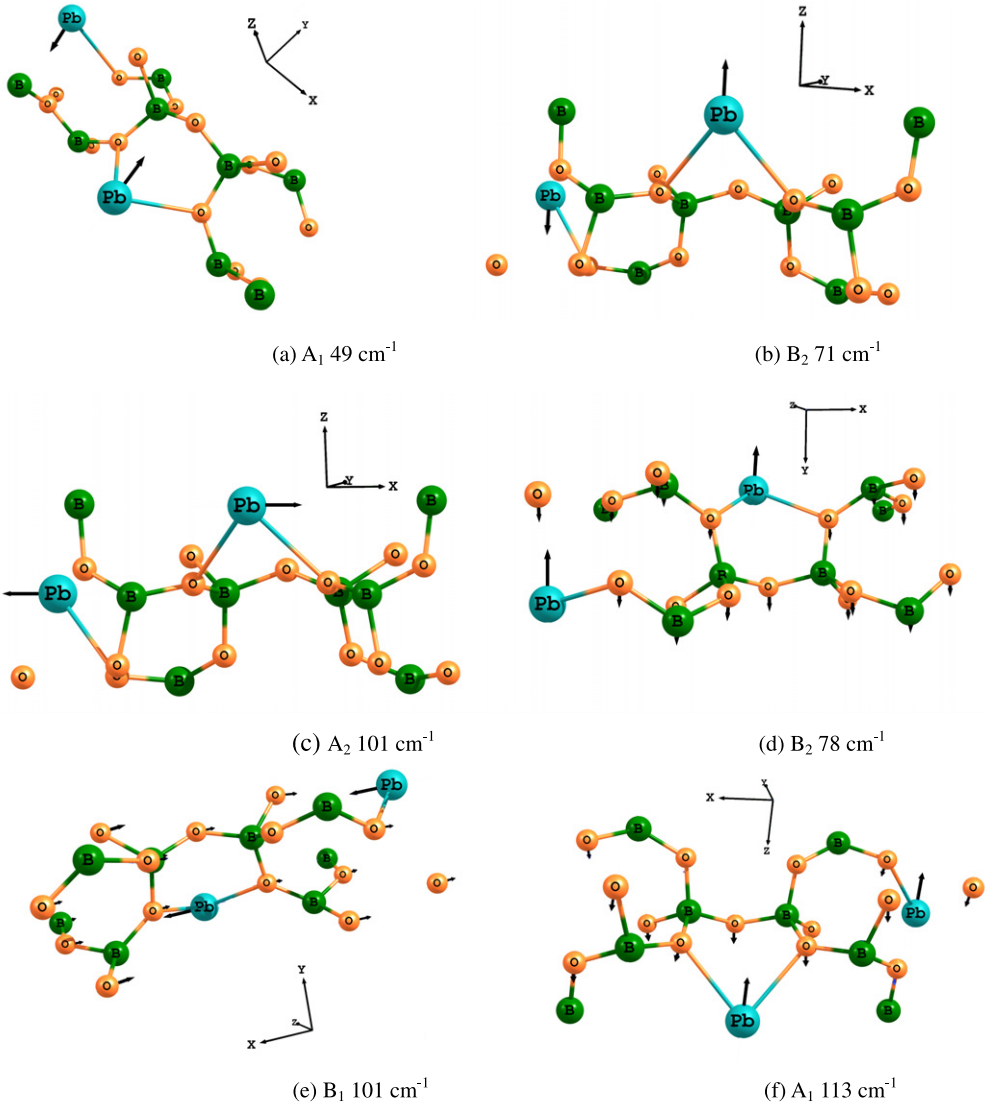

(a) A_1 49 cm^{-1} (b) B_2 71 cm^{-1}

(c) A_2 101 cm^{-1} (d) B_2 78 cm^{-1}

(e) B_1 101 cm^{-1} (f) A_1 113 cm^{-1}

Figure 6. Cartesian displacements of atoms in vibrational modes of PTB crystal. The frequencies are the calculated data.

4.5. Discussion

According to references [7, 8], the structural unit of PTB crystal cannot be considered as either BO_4 tetrahedra or $(B_3O_9)^{9-}$ six-membered rings. For borate crystals consisting of six-membered rings with one or two BO_4 tetrahedra, there is a very strong Raman peak near 770 cm^{-1} [16]. But no such vibrational band exists in the Raman spectra of PTB crystal. It is more reasonable for lead tetraborate to be considered as consisting of BO_4 tetrahedra rather than $(B_3O_9)^{9-}$ six-membered rings. As an approximation one can assign the high-frequency modes to the BO_4 tetrahedra.

According to the literature [17], the highest vibrational frequency is an important indirect indication of the nonlinear optical activity for borate crystals. Generally, the highest vibrational

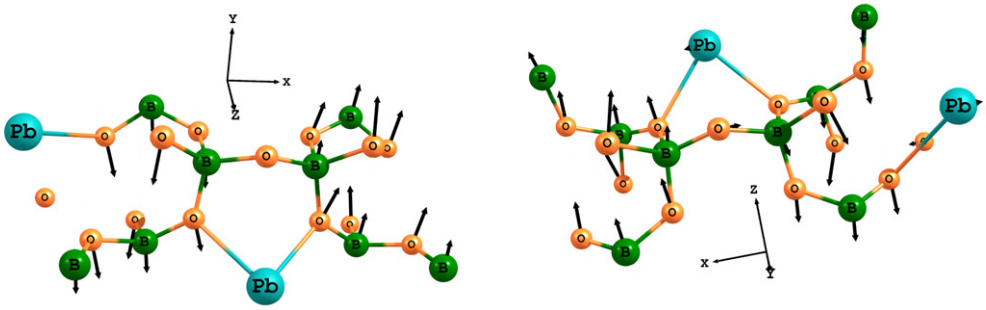

(a) B_1 166 cm^{-1} (b) A_2 178 cm^{-1}

Figure 7. Cartesian displacements of atoms in vibrational modes of PTB crystal. The frequencies are the calculated data.

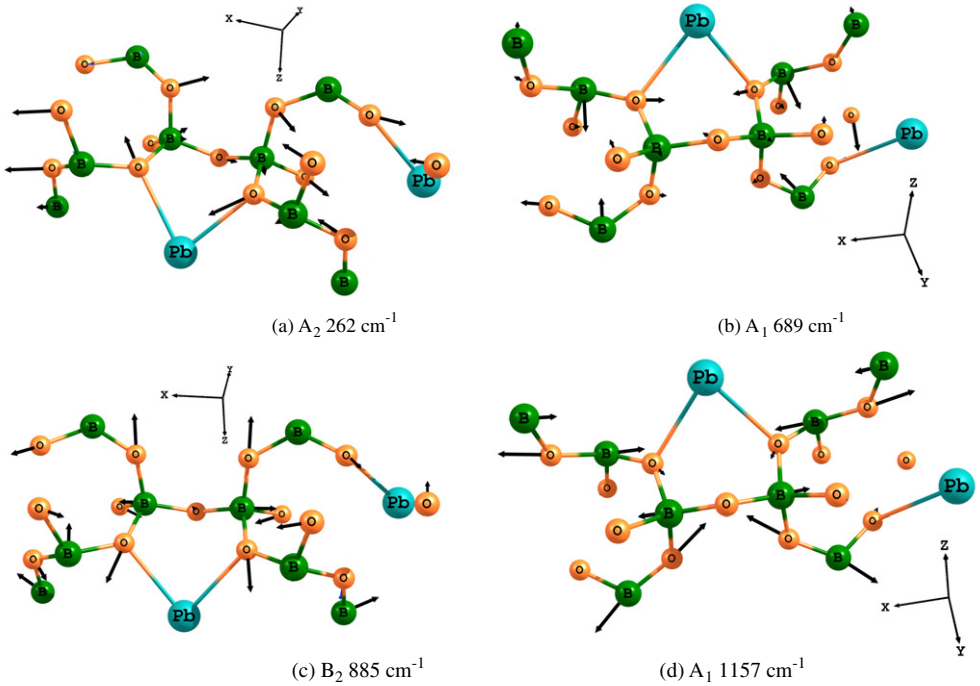

(a) A_2 262 cm^{-1} (b) A_1 689 cm^{-1}

(c) B_2 885 cm^{-1} (d) A_1 1157 cm^{-1}

Figure 8. Cartesian displacements of atoms in vibrational modes of PTB crystal. The frequencies are the calculated data.

frequency of a crystal with large optical nonlinearity is also large. In β-BaB_2O_4, LiB_3O_5, $CsLiB_6O_{10}$ and CsB_3O_5 crystals, for example, large nonlinear optical activities have been observed [18–22]. Their basic structural units are six-membered rings or six-membered rings with one BO_4 tetrahedron. According to the 'anion group theory' [18], the large nonlinear optical activities of these crystals were attributed to the $(B_3O_6)^{3-}$ or $(B_3O_7)^{5-}$ units, the highest vibrational frequency of which exceeds 1500 cm^{-1} [1–5]. In PTB crystal, which only contains BO_4 tetrahedral groups, the highest vibrational band observed does not exceed 1200 cm^{-1}. According to the 'anion group theory' [23] the optical nonlinearity of PTB crystals is low. But according to Nicholls *et al* [6], the nonlinear optical coefficients of PTB is larger than those

of BBO and LBO which contain $(B_3O_6)^{3-}$ or $(B_3O_7)^{5-}$ groups, respectively. Therefore, the enhanced nonlinear optical response of PTB cannot be associated with boron–oxygen units. The vibrational spectra of PTB crystal show that there exist strong vibrational bands in the low-frequency region, which are due to the contribution of Pb atoms. According to the bond charge model [24], the nonlinear optical properties of a complex crystal may be regarded as a combination of all constituent chemical bonds, i.e., the macroscopic tensor elements of the nonlinear susceptibilities can be expressed as an appropriate sum over the contributions of single bonds. In a highly symmetrical bonding configuration, the contributions of single bonds will tend to cancel (or partially cancel) each other and hence cause a low optical nonlinearity. Similarly, highly asymmetric bonding leads to significantly less cancellation and hence a greater nonlinearity. In PTB the Pb sites are highly distorted, with seven-fold coordination to the nearest O atoms. The five shortest Pb–O bonds lie to one side of the Pb atom, while the remaining two longer bonds are on the opposite side. Moreover, the Pb^{2+} ions have high polarizabilities. Therefore, it is reasonable assume that the dominant contribution to the nonlinear optical response of PTB may be associated with the highly polarizable Pb^{2+} ions in the highly distorted lattice sites [8]. Certainly, this assumption needs further investigation.

5. Conclusions

In the present study, Raman and infrared spectra of PTB at room temperature have been measured. The phonon dispersion has been calculated based on first principles. The calculated vibrational frequencies at the centre of the Brillouin zone are in good agreement with experimental data. Pb atoms mainly contribute to the vibrations with frequencies below 166 cm^{-1}. The complex character of the crystal structure of PTB is reflected in the complexity of the vibrational spectra.

References

[1] Wang Y F, Lan G X and Wang H F 1992 *Spectrochim. Acta* A **48** 181
[2] Ney P, Fontana M D, Mailard A and Polgar K 1998 *J. Phys.: Condens. Matter* **10** 673
[3] Wang Y, Liu J, Hu S, Lan G, Fu P and Wang Z 1999 *J. Raman Spectrosc.* **30** 519–23
[4] Xiong G, Lan G and Wang H 1993 *J. Raman Spectrosc.* **24** 785–9
[5] Wang Y, Liu J, Hu S and Lan G 1999 *Spectrochim. Acta* A **55** 2565–71
[6] Nicholls J F H, Chai B H T, Ressell D and Henderson B 1997 *Opt. Mater.* **8** 185–91
[7] Perloff A and Block S 1966 *Acta Crystallogr.* **20** 274–9
[8] Corker D L and Glazer A M 1996 *Acta Crystallogr.* B **52** 260–5
[9] Hohenberg P and Kohn W 1964 *Phys. Rev.* **136** B864
[10] Kohn W and Sham L J 1965 *Phys. Rev.* **140** A1133
[11] Payne M C, Teter M P and Allan D C 1992 *Rev. Mod. Phys.* **64** 1045
[12] Hamann D R, Schluter M and Chiang C 1979 *Phys. Rev. Lett.* **43** 1494
[13] Baichelet G B, Hamann D R and Schluter M 1982 *Phys. Rev.* B **26** 4199
[14] Monkhorst H J and Pack J 1976 *Phys. Rev.* B **13** 5188
[15] Zhigadlo N D, Zhang M and Salje E K H 2001 *J. Phys.: Condens. Matter* **13** 6551
[16] Bril T W 1976 *Philips Res. Rep. Suppl.* **31** 1
[17] Shang Q Y, Hudson B S and Huang C E 1991 *Spectrochim. Acta* **47** A291
[18] Chen C 1989 *Laser Focus World* **25** 129
[19] Wu Y, Sakaki T, Nakai S, Yokotani A, Tang H and Chen C 1993 *Appl. Phys. Lett.* **62** 2614
[20] Mori Y, Kuroda I and Nakajima S 1995 *J. Cryst. Growth* **156** 307
[21] Mori Y, Kuroda I, Nakajima S, Sakaki T and Nakai S 1995 *Japan J. Appl. Phys.* **34** L296
[22] Mori Y, Kuroda I, Nakajima S, Sasaki T and Nakai S 1995 *Appl. Phys. Lett.* **67** 1818
[23] Heyna A M, Range K J and Wildenauer M 1990 *Spectrochim. Acta* A **46** 1621
[24] Levine B F 1973 *Phys. Rev.* B **7** 2600